The significance of endothelial stomata and stigmata in the rat aorta

An electron microscopic study

Guido Majno, Jean M. Underwood, Thomas Zand, and Isabelle Joris
Department of Pathology, University of Massachusetts Medical School,
55 Lake Avenue North, Worcester, MA 01605, USA

Summary. Perfusion of arteries with dilute silver nitrate produces in the endothelium (a) a pattern of pericellular black lines, which we earlier interpreted as a marker of the physiological electrolyte pathway (Zand et al. 1982), and (b) focal black deposits on or between the cells, either ring-shaped (*stomata*) or solid (*stigmata*). The purpose of this study was to clarify the nature and significance of these controversial structures. A glutaraldehyde-fixed *normal* rat aorta was perfused with silver nitrate; 17 typical stomata and stigmata were photographed *en face*, then studied on ultrathin serial sections. When seen *en face*, they fell into three groups: (I) 4 stomata in endothelial cells; (II) 6 stigmata in endothelial cells; (III) 7 stigmata on intercellular junctions. By electron microscopy, (I) all the *stomata in endothelial cells* corresponded to myoendothelial herniae. (II) Of the 6 *stigmata in endothelial cells*, 4 corresponded again to myoendothelial herniae, 2 corresponded to blebs (it seemed likely that these blebs had existed *in vivo*, but the possibility of a fixation artefact could not be excluded). (III) Of the 7 *stigmata on intercellular junctions*, one corresponded to the diapedesis of a mononuclear cell; the other 6 did not correspond to visible endothelial changes and are best interpreted as points of normally higher permeability. We conclude that stomata and stigmata (under the conditions of our experiments) can be explained in at least 4 different ways, depending in part on their location (in cells, on junctions). These ancient terms therefore remain useful for descriptive purposes, as long as it is realized that their significance in any given case must be determined by electron microscopic study.

Key words: Stoma – Stigma – Myoendothelial hernia – Diapedesis – Permeability

---

Offprint requests to: G. Majno at the above address

Introduction

One of the endothelial puzzles that still persists is the significance of the so-called *stomata* and *stigmata*: traditional names for focal deposits of black metallic silver (ring-shaped or solid, respectively) seen by light microscopy in blood vessels treated with a dilute solution of silver nitrate and examined *en face*. The dilemma is practically as old as the silver method: the first to discuss the possible significance of intercellular stomata was His in 1863 (Stadtmüller 1921). Two questions arose: (a) do these structures represent microscopic leaks, as both names imply, and (b) are they real structures or artifacts of the technique? Both questions should be answered, because stomata and stigmata play a role also in pathology, as ever-present components of vascular disease (Altschul 1954; Stehbens 1965; Fallon and Stehbens 1973; Caplan et al. 1974; Silkworth et al. 1975).

A systematic study of *mesothelial* stomata by light and electron microscopy has proven beyond doubt that they represent complex physiologic structures (Leak and Rahil 1978; Mironov et al. 1979; Tsilibary and Wissig 1983). There has been no comparable study at the level of the endothelium, possibly because electron microscopy of normal arterial and venous endothelium has not shown intercellular gaps, which suggests that "leaks" shown by the silver method may be artifacts.

It seemed to us that the most direct way to settle the matter was to treat a vessel with silver nitrate, identify stomata and stigmata by light microscopy, then cut each one serially for study by electron microscopy. The approach is very time-consuming and requires a compromise as regards the quality of ultrastructure, because silver nitrate (even if applied after glutaraldehyde fixation) causes some focal disruption. However, this must be the first step: it is the purpose of this paper. We chose to study the aorta of the rat, because this vessel is widely used also for the study of experimental atherosclerosis (Joris et al. 1983).

Terminology. Respecting the traditional usage, we will restrict the term *stoma* (mouth) to ring-shaped structures with a clear (or clearer) center. *Stigma* will refer to deposits that appear as solid black dots, with or without a halo of finer granules. *It will be understood that both stomata and stigmata may occur on the endothelial cells or on the silver lines.*

Materials and methods

Silver lines were produced in the aorta of a healthy 250 g Wistar rat (Charles River Laboratories, Wilmington, MA, USA) according to the method of Zand et al. (1982). Briefly: a 20 min supravital perfusion with 3% glutaraldehyde at 110 mm Hg is followed by 1 min perfusion with 0.05% silver nitrate, 1 min perfusion with bromides, then exposure to light in glutaraldehyde for a total fixation time of 5 h. A ring of the silvered upper abdominal aorta was post-fixed in 1.3% OsO_4 in 0.1M cacodylate buffer at 4° C for 1 h, rinsed in cacodylate buffer, dehydrated in graded ethanols and propylene oxide, then infiltrated in Epon 812 (E. Fullam, Inc., Schenectady, NY, USA). Just prior to embedding, the aortic ring was recut into many tiny, narrow pieces with a razor blade. These were sandwiched between two disposable plastic coverslips (Fisher Scientific Co., Pittsburgh, PA, USA) in a very thin layer of Epon which was then
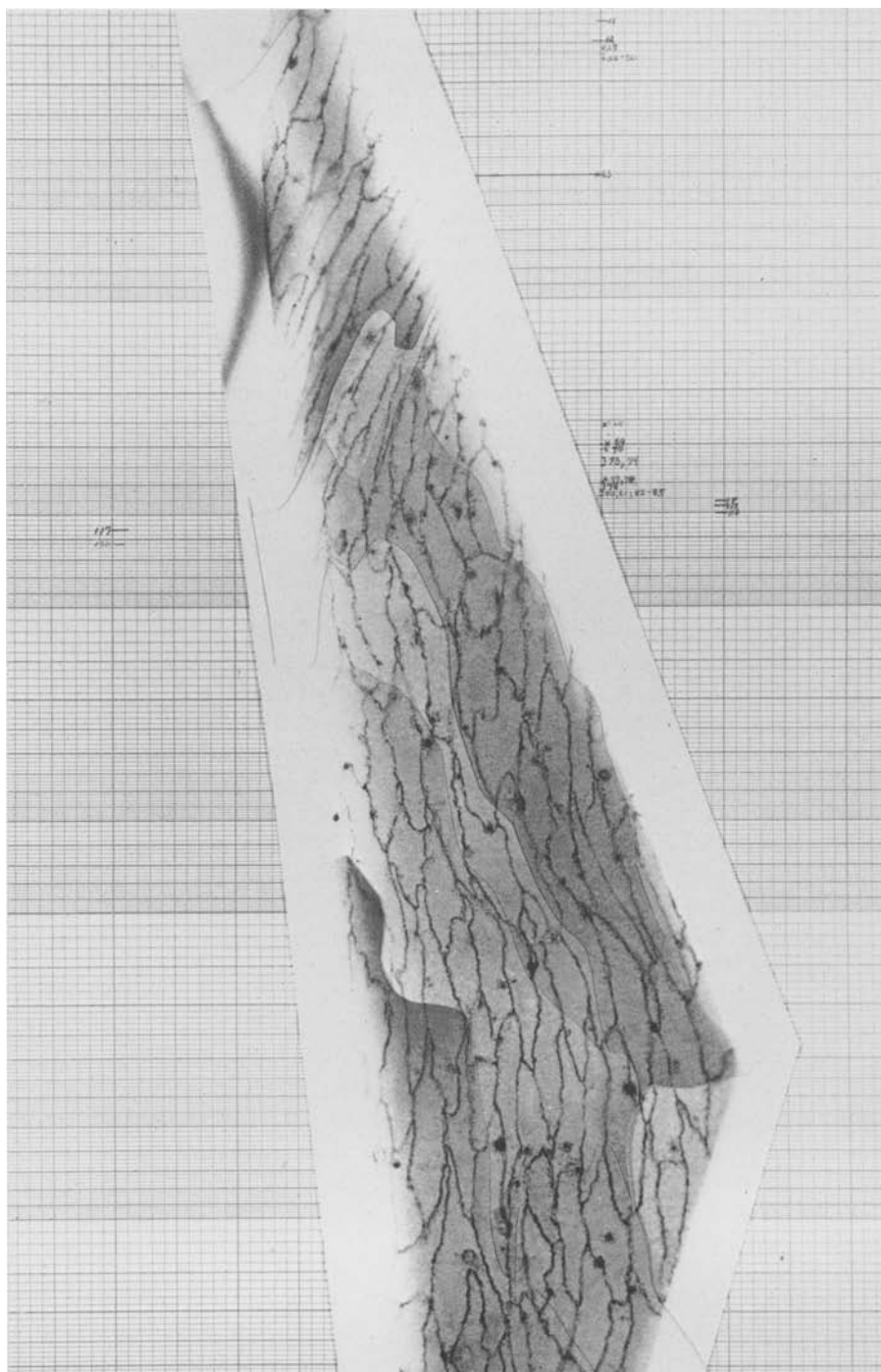
Fig. 1. Montage of light micrographs, showing the principal block that was serially sectioned. Silver nitrate method, flat embedding in Epon. Stomata and stigmata are visible (shown in detail in Fig. 2) (310 ×)

polymerized. Each block of tissue was scanned *en face* under the light microscope for the presence of both stomata and stigmata. Two pieces of tissue were ultimately selected for serial sectioning because they contained typical examples of each. They were narrow strips only 2–21 cells in width. Each block was then taped to a glass slide and photographed *en face* with a Zeiss Photomicroscope II. For each strip of tissue, photographs were assembled into a montage (referred to hereafter as *topographic view*), which was glued over a sheet of ruled paper on which the cutting plane was logged (Fig. 1).

One of the plastic coverslips was peeled off, and sections were cut through the remaining plastic coverslip and the tissue adherent to it. Thick sections were cut with glass knives, and thin sections with a diamond knife on an LKB Ultrotome III. Every section kept was assigned a number. As cutting progressed, the topography of the sections was controlled by comparing the topographic view with the light microscopic examination of the block. Thin sections were picked up on formvar coated slot grids and stained with lead citrate. These serial thin sections were systematically examined with a Philips 301 electron microscope. Representative section levels were photographed at low magnification, and montages of the entire intimal surface in cross section were made. Cell junctions (visible as black silver deposits) were continually counted – proceeding from the edge of the block inwards – to correlate the cells seen by electron microscopy with those appearing on the topographic view; thus they were used as reference points for locating stomata and stigmata. When one of these was positively identified, it was serially sectioned and photographed at higher magnification.

Results

The topographic view of the principal block selected for our study is shown in Fig. 1. It contained about three dozen structures that could be classified as stomata or stigmata as defined above. We selected the 16 that were morphologically best defined; they were sequentially numbered (in topographic sequence) and each one was cut in serial ultrathin sections. The second block showed the same structures and was handled in the same manner as the first (only one stigma was identified). Preliminary results showed that the 17 chosen stomata/stigmata differed in significance not only depending on their structure (rings or dots) but also depending on their location (inside the cells, on the junctions) (Fig. 2). We will therefore describe separately both stomata and stigmata that occurred "inside the cells" or "on the junctions".

(a) *Stomata* always fell inside cells; in this material, none were found along junctions. The 4 structures of this kind (Fig. 2, Nos. 3, 4, 10 and 15) were 5.8, 4.4, 3.6 and 6.3 microns in diameter. In ultrathin sections, all 4 corresponded to a myo-endothelial hernia (Stetz et al. 1979), either bulging or collapsed. For example, No. 3 seen *en face* was an oblong stoma (Fig. 2, no. 3). In serial sections it corresponded to a myoendothelial hernia causing the endothelium to bulge; part of the bulge had collapsed into a cup-shape (Fig. 3). Silver grains had precipitated unevenly along the contour and the bottom of the hernia (Fig. 4).

(b) *Stigmata in the cells*. Of 6 structures of this kind, 4 corresponded – again – to myoendothelial herniae (Fig. 2, Nos. 2, 7, 12, 17). As seen *en face*, their diameters were 3.4, 3.6, 2.0 and 5.1 microns. A typical example is No. 2 (Fig. 2); in ultrathin sections the hernia was intraendothelial (Fig. 5); it was collapsed, and the black smudge of silver seen *en face* corresponded to a subendothelial pool of silver grains beneath the hernia (Fig. 6);
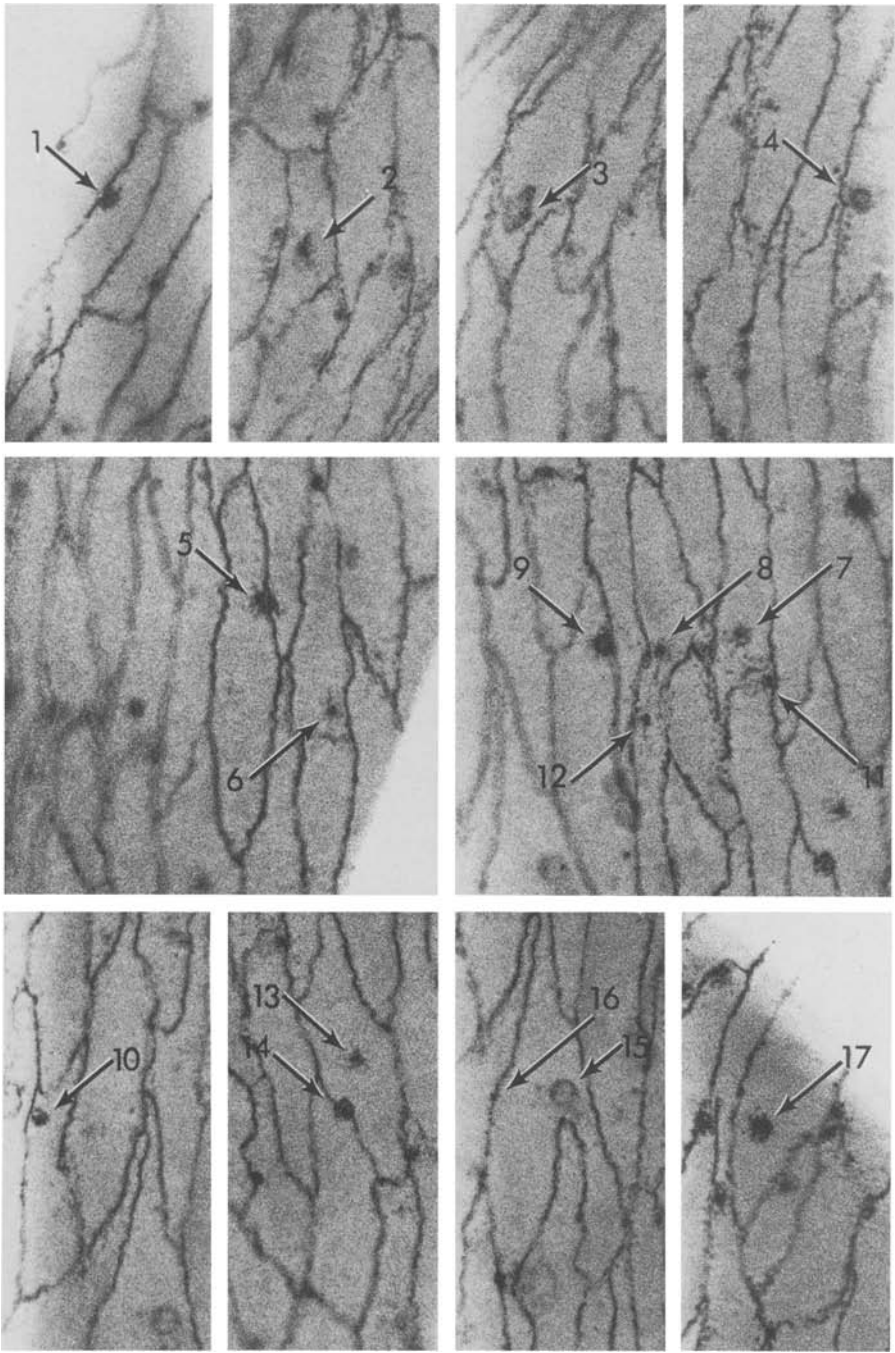
Fig. 2. Rat aorta after silver nitrate staining and flat embedding. Detailed view of the 17 stomata and stigmata selected for serial sectioning. Classified as stomata (rings) were 3, 4, 10, and 15; the ring structure – best seen by focusing – is obvious in Nos. 4 and 15 (620 ×)
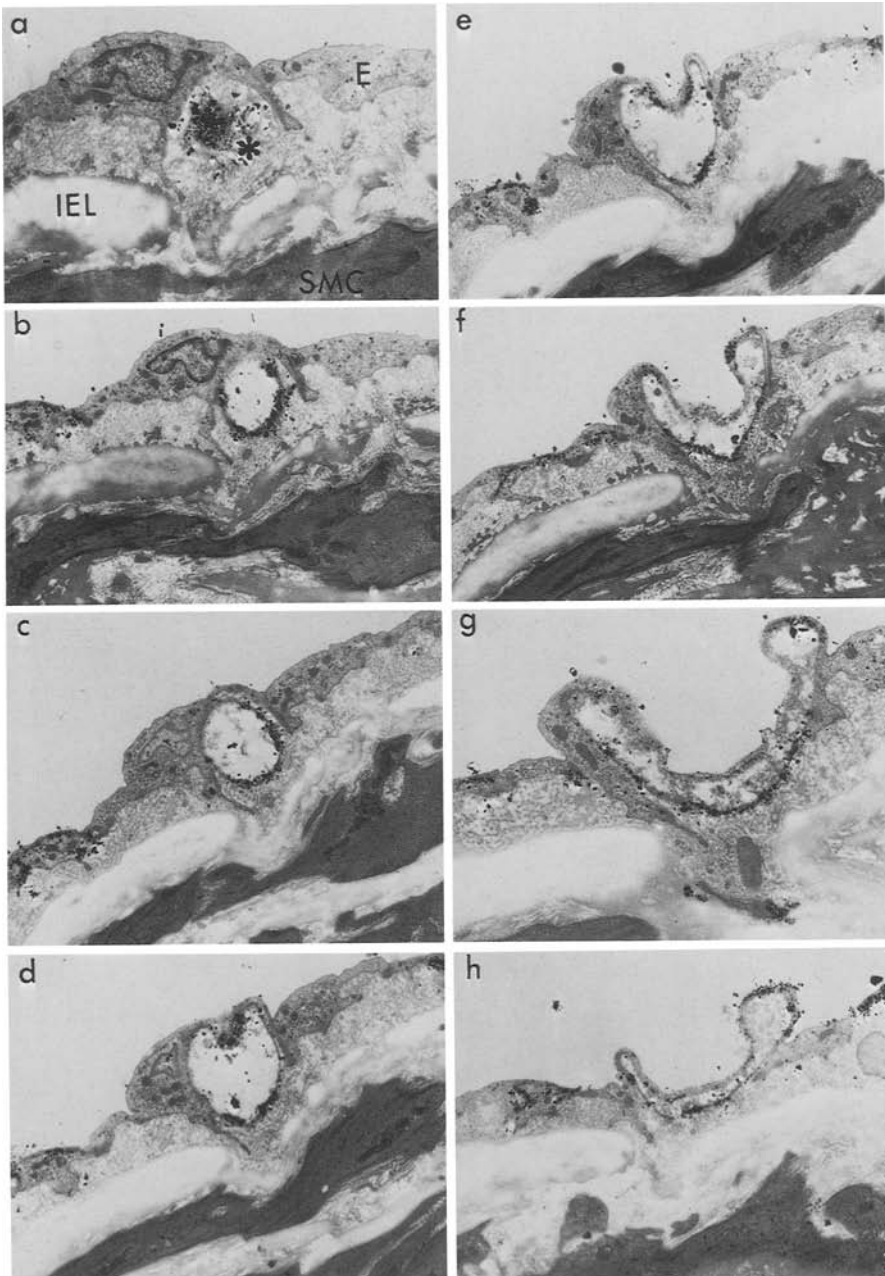
Fig. 3. Stoma (No. 3) as seen by electron microscopy at different serial levels. A myoendothelial hernia (∗) causes the endothelium (*E*) to bulge into the lumen (**a–c**), then collapses into a cup-shape (**d–h**). Note silver deposits along the contour of the myoendothelial hernia and on the interendothelial junctions. *IEL*: internal elastic lamella; *SMC*: smooth muscle cell (**a** = 7,120 × ; **b–f**, **h**) = 5,890 × ; **g** = 9,720 ×)
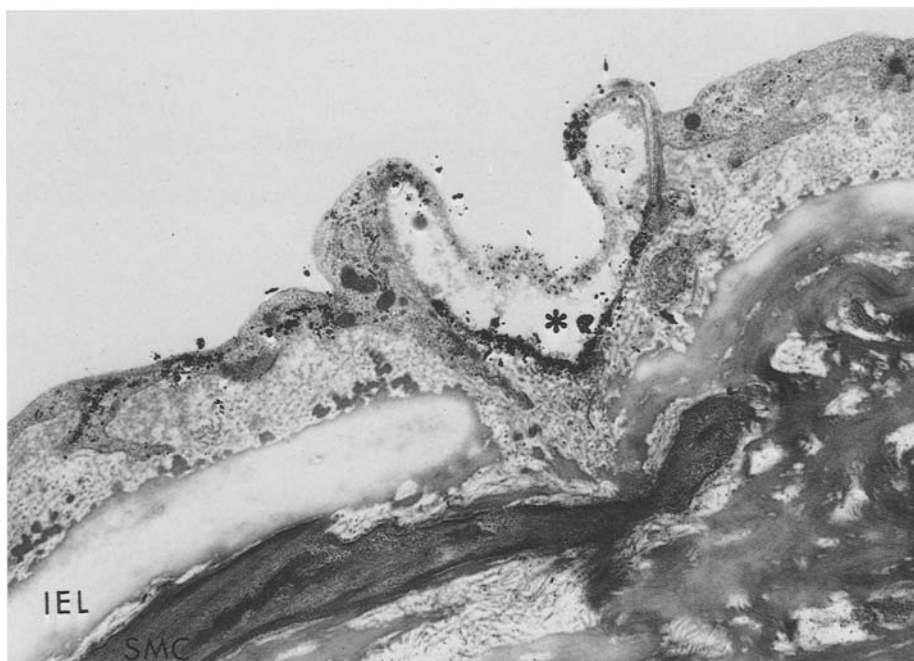
Fig. 4. Stoma No. 3, detail. Silver grains are deposited along the base of the myoendothelial hernia (∗) and in clumps on its luminal surface. The presence of silver not only on the edges but also on the bottom of this myoendothelial hernia explains why, seen *en face* (Fig. 2), this stoma appeared diffusely grey and not clearly ring-shaped. *IEL*: internal elastic lamella; *SMC*: smooth muscle cell (12,560 ×)

No. 7 (Fig. 2) corresponded to another cup-like hernia open to the lumen; clusters of silver granules had formed just beneath its opening (Fig. 7). No. 17 (Fig. 2) showed that the silver grains formed a large deposit over the top of the hernia and on its sides (Fig. 8a and b).

Two of 6 stigmata "in the cell" gave a different result (Fig. 2, Nos. 6, 13). Seen *en face*, their diameters were 1.9 and 2.9 microns. By EM they corresponded to a cluster of silver granules on a multivesicular bleb arising from the endothelial cell membrane; some additional silver deposit was present just *beneath* the multivesicular bleb (Fig. 9).

Stigmata on the junctions were 7 (Nos. 1, 5, 8, 9, 11, 14, 16). Fig. 2 shows their typical appearance *en face* (diameters: 3.6, 5.6, 2.3, 4.8, 2.3, 4.3, and 1.4 microns). By EM, all but one (No. 16) had a uniform aspect: large silver deposits in connection with an intercellular junction (on it, beneath it, and irregularly in the adjacent cell cytoplasm). An example is shown in Fig. 10. The surface of the endothelium in the area of the deposit occasionally showed simple myelin figures or multivesicular blebs. No subendothelial herniae were present. Stigma 16 was discovered *a posteriori*: serial sectioning revealed a monocyte performing diapedesis (Fig. 11a, b). Silver granules impregnated the "tail" of the monocyte protruding into
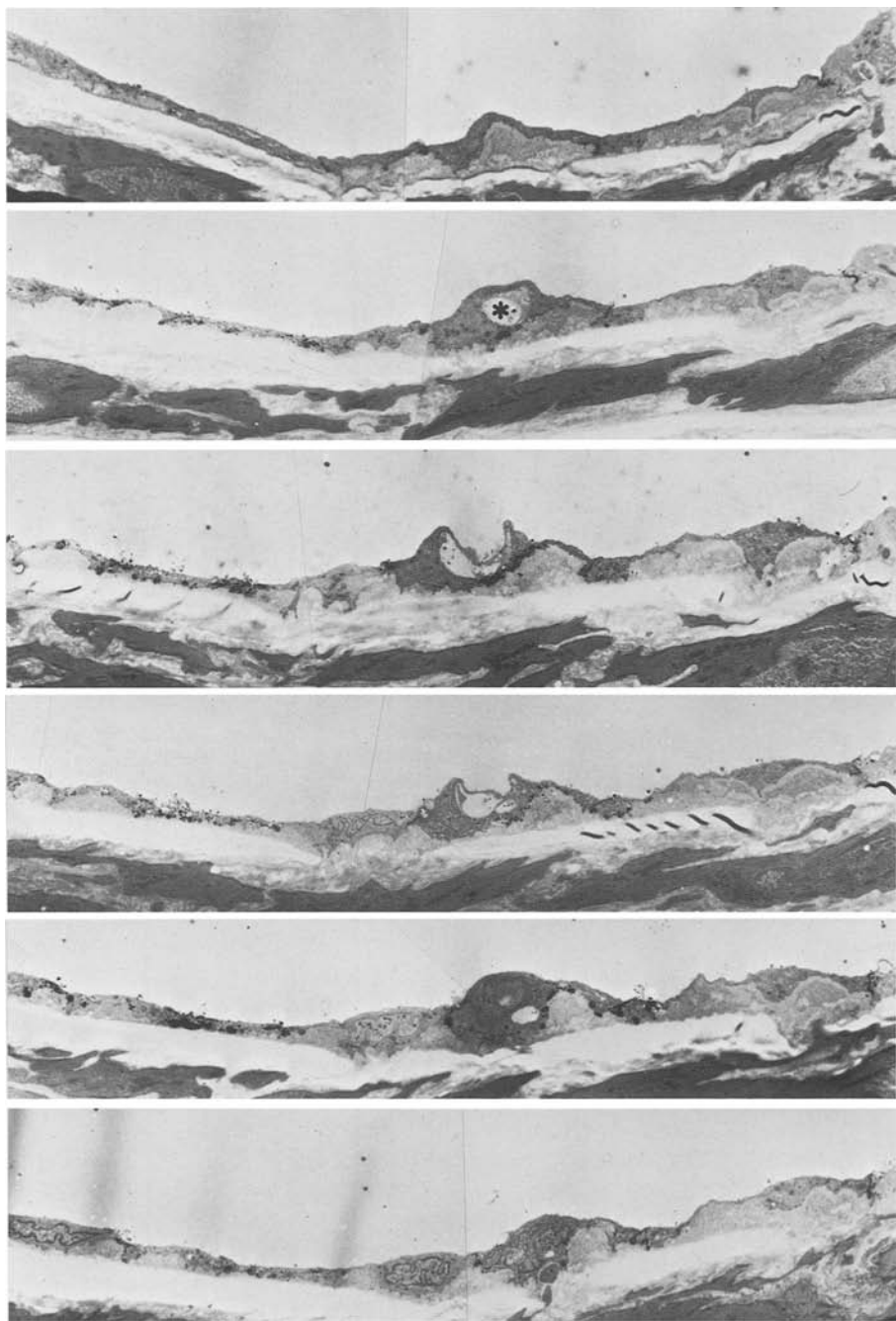
Fig. 5. Representative sections through stigma No. 2. A myoendothelial hernia (∗) is seen as an intraendothelial structure causing the endothelium to bulge into the lumen. Silver grains are deposited beneath it (2,460 ×)
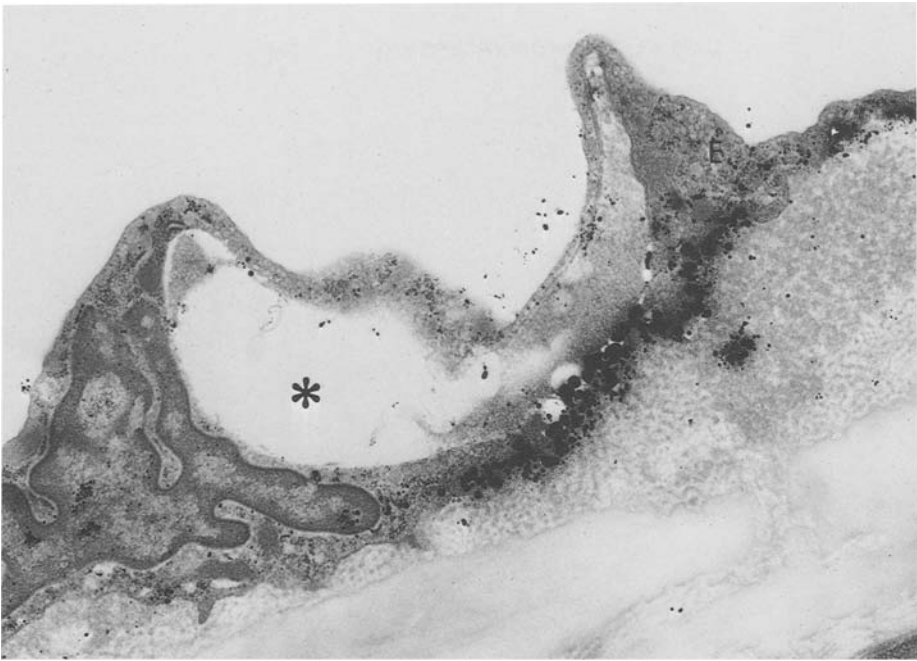
Fig. 6. Stigma No. 2, detail. Note the massive silver deposit at the level of the basement membrane, beneath the myoendothelial hernia (*). This topography of the silver deposit explains the appearance of this stigma *en face* (Fig. 2): a solid black mass rather than a ring. E=endothelium ($20,340 \times$)
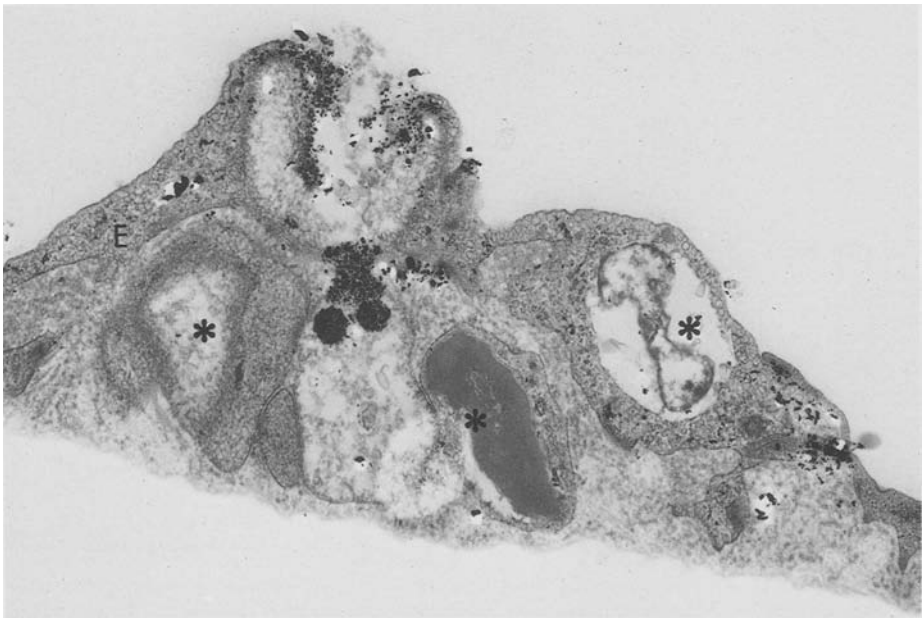

Fig. 7. Section through stigma No. 7 showing a cup-shaped hernia open to the lumen; silver deposits have clustered just below its opening. (Note other herniae (*) in the endothelium (E) and beneath it.) The silver deposits occur mainly in the center of the hernia, explaining its appearance *en face* as a solid black mass (Fig. 2) ($15,070 \times$)
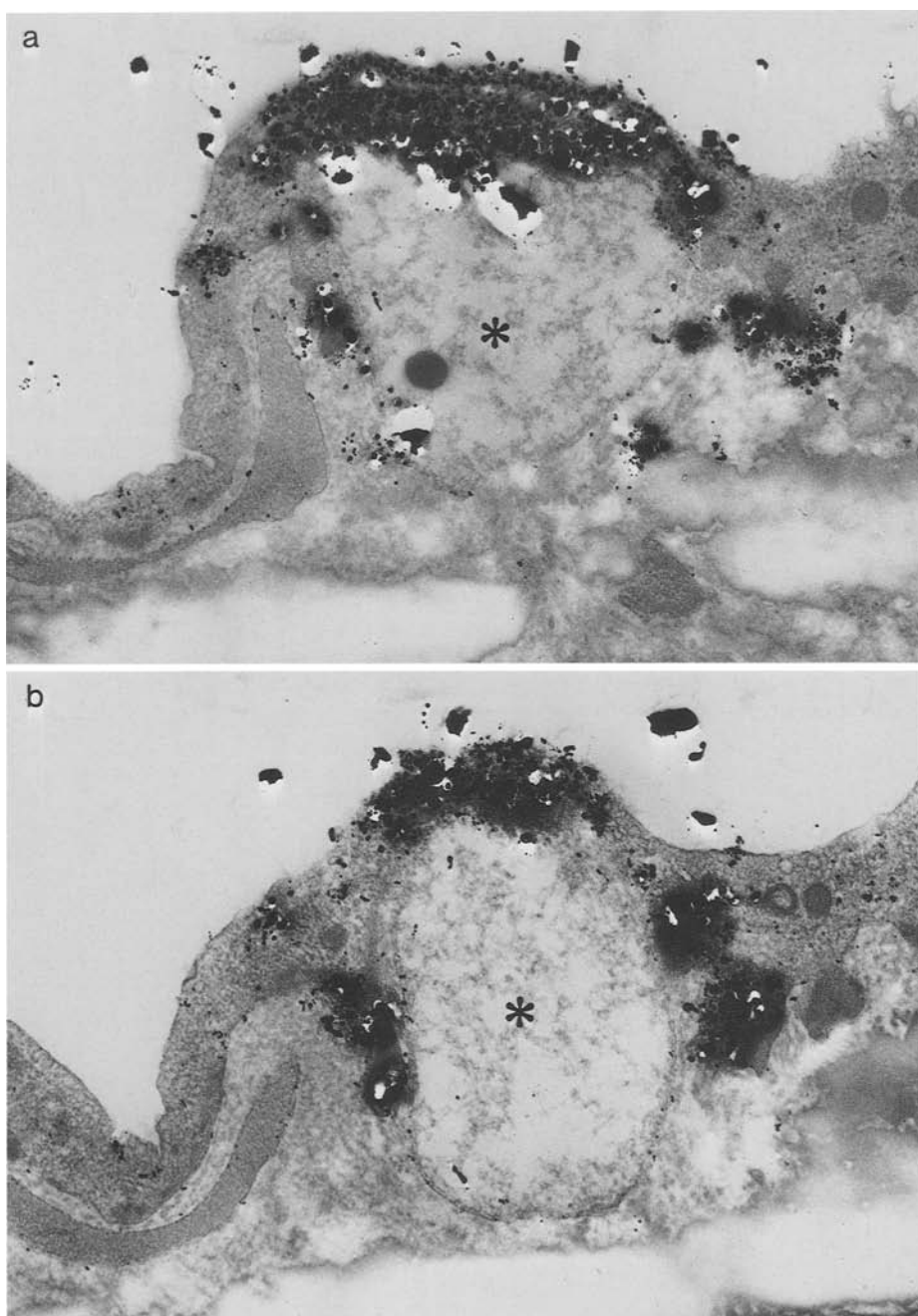
Fig. 8. Sections at two different levels through stigma No. 17. There is a myoendothelial hernia (∗) with heavy silver deposits on its top (**a**), as well as along its sides (**b**). These lateral deposits alone, seen *en face*, would have produced the appearance of a ring; but the ring was filled by the massive "top" deposits, hence this hernia took on the appearance of a solid black mass (22,800 ×)
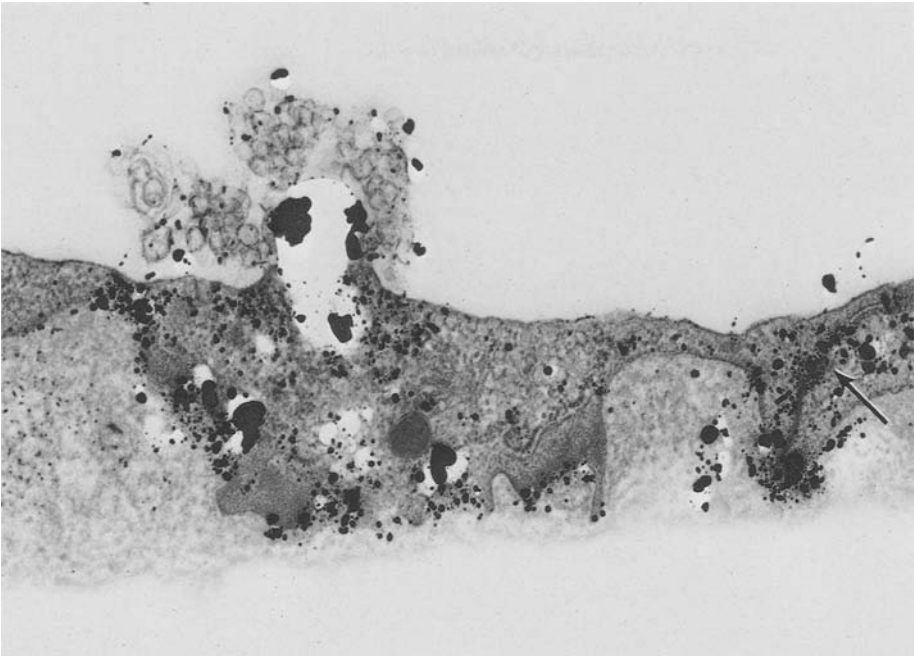
Fig. 9. EM appearance of stigma No. 6. On the right, note silver deposits in and beneath a junction (arrow): this is the silver line visible in Fig. 2 near stigma No. 6. The stigma itself corresponds to a multivesicular bleb arising from the endothelial surface, with moderate silver deposits in and beneath the endothelium ($28,820 \times$).
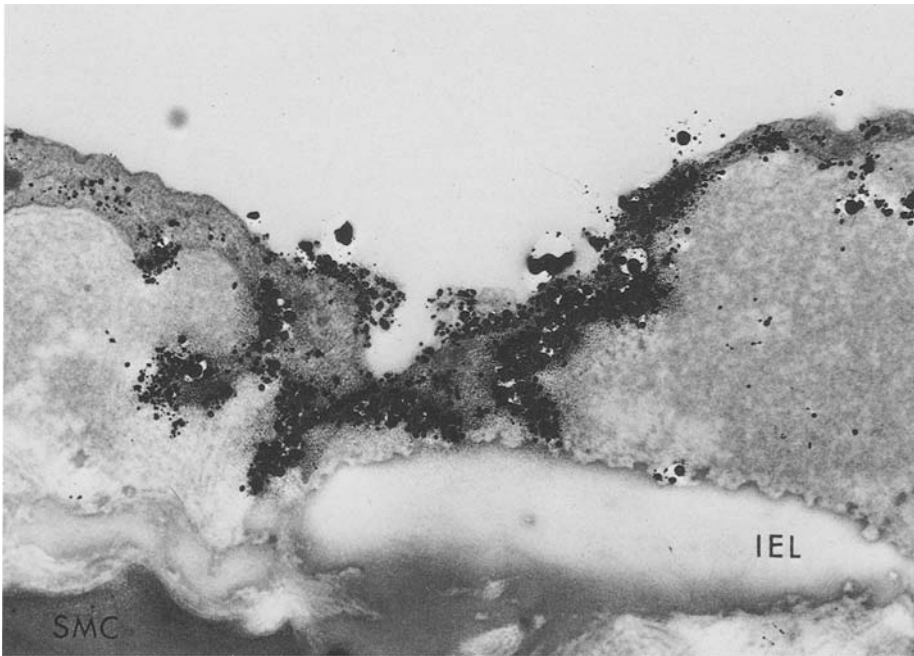

Fig. 10. EM appearance of stigma No. 5, which – seen *en face* – was astride a silver line (Fig. 2). Extensive silver deposits, predominantly beneath the endothelium, on one side of a junction. No myo-endothelial hernia is present (*IEL*: internal elastic lamella; *SMC*: smooth muscle cell) ($14,810 \times$)
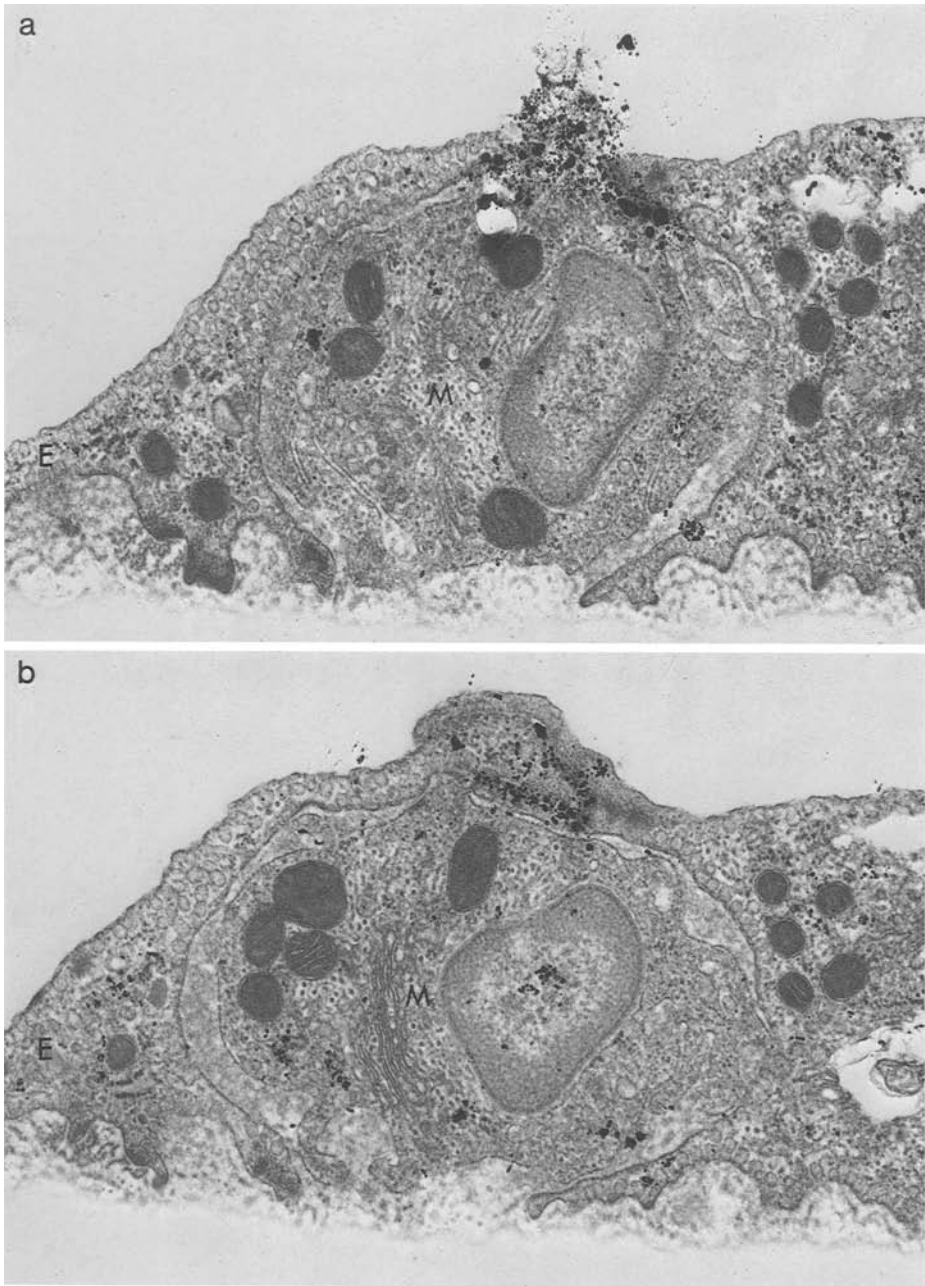
Fig. 11. Serial sections through a monocyte (*M*) performing diapedesis between two endothelial cells (*E*). This level corresponds to stigma No. 16 as seen *en face* (Fig. 2). (**a**) At this level the uropod of the monocyte is still protruding into the lumen. The seal between endothelium and monocyte was not tight enough to prevent some silver nitrate from trickling into the intercellular space. (**b**) At a deeper level the monocyte appears completely covered by endothelium, beneath a junction (marked by silver grains) (28,380 ×)

the lumen (Fig. 11 a) and 4 microns away they delineated the closed junction (Fig. 11 b). Seen *en face* this monocyte corresponded to a dot on a silver line, so small that it had previously escaped our attention (Fig. 2, No. 16).

Discussion

In our material (limited to the *normal* rat aorta) a selection of 17 stomata and stigmata corresponded to at least four types of electron microscopic findings.

Eight corresponded to typical myoendothelial herniae. These structures are created by a long pseudopod arising from a medial smooth muscle cell lying just beneath the elastica interna, and reaching the subendothelial space through a fenestra or from a smooth muscle cell lying just above the internal elastic lamella (Hoff and Gottlob 1967; Stetz et al. 1979). The swollen extremity of the pseudopod bulges beneath the endothelium, and stretches it to such thinness that it is sometimes perforated (Stetz et al. 1979). When prepared for scanning EM these bulges tend to collapse into the shape of craters, often described in arterial endothelia (Edanaga 1974; Gregorius and Rand 1975; Gertz et al. 1976; Gordon et al. 1981). An earlier view, based on light microscopic studies (Björkerud et al. 1972), proposed that endothelial stomata in the rabbit aorta are physiologic "valves". This interpretation cannot be maintained. The careful descriptions of these authors suggest that they were observing collapsed myo-endothelial herniae.

When seen *en face*, of the 8 myoendothelial herniae, 4 appeared more or less obviously as a black ring (stoma) in the endothelial cell, and 4 as a stigma also in the cell. We must now explain (a) why the silver precipitates at the site of the myoendothelial herniae, and (b) why, seen from above, the deposit is either a black ring or a black dot. We can offer an answer, based on detailed study of the serial EM sections, and on previous experience with the electron microscopy of the silver method (the masses of silver grains seen by EM must be understood as greatly extended "outgrowths" of original, much more discrete primary deposits (Zand et al. 1982). Our explanation is summarized in Fig. 12: silver ions traverse the stretched, extremely thin endothelium overlying a hernia (where the thickness of the endothelial cell can be of the order of one plasmalemmal vesicle or less). Once the silver reaches the space between the endothelium and the smooth muscle cell pseudopod it encounters basement membrane material, which causes it to precipitate (basement membranes being argyrophilic). The aspect of the precipitate as seen from above will then depend on the site of the major deposit: if most of the black granules are on the sides of the hernia, the view from above will show a ring; if the deposit is collected mainly at the top or at the base of the hernia, it will appear as a black dot. The difference may well be random.

Our interpretation is supported by the fact that serial sectioning found several myo-endothelial herniae that did not correspond to any silver deposit: in all these cases the herniae were too small or too far below the surface to stretch the endothelium.
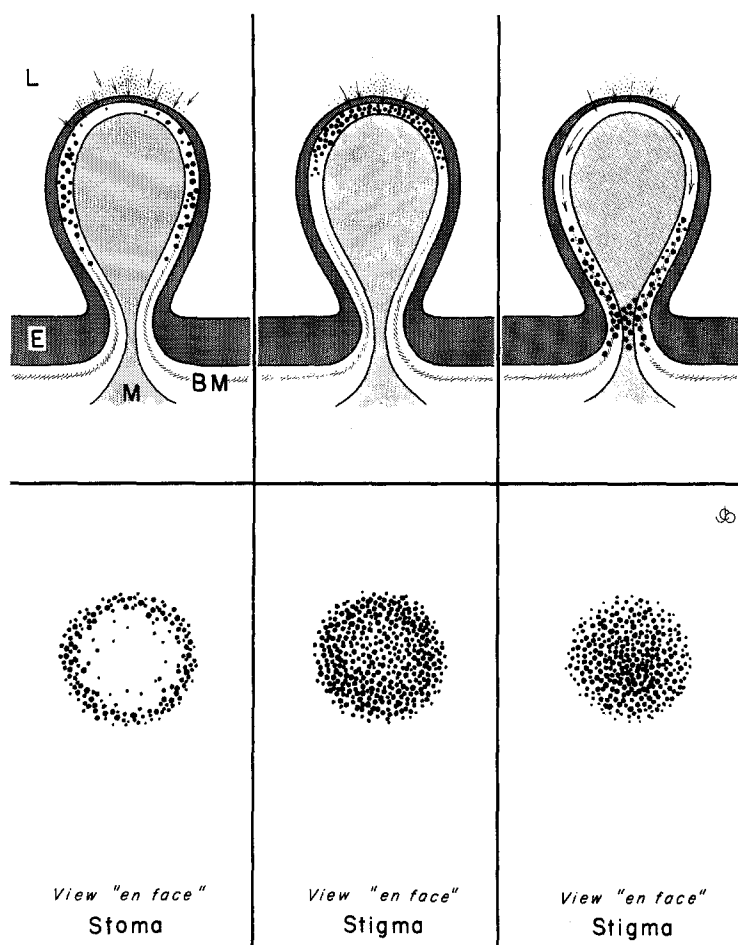
Fig. 12. Scheme of the mechanisms whereby myoendothelial herniae can give rise (after perfusion with silver nitrate) to the appearance of either a stoma or a stigma. The endothelial bulge over the hernia is drawn as a rounded shape, but in fixed tissues it often appears collapsed into a cup-shape or crater. The small dots in the lumen (L) represent ions of silver nitrate, which penetrate through the thinner endothelium and give rise to grains of metallic silver (black spots). (E = endothelium, BM = basement membrane, M = protrusion of smooth muscle cell (myoendothelial hernia)). See text

Two of 6 stigmata in endothelial cells did not correspond to any distinct preexisting lesion. They appeared as a mass of silver lying in and beneath the endothelial cell, with small myelin figures arising from the luminal surface of the endothelium (Fig. 9). Occasional myelin figures do arise from normal endothelium (Joris et al. 1982) or after mild injury (Gertz et al. 1976; Joris et al. 1982); it is conceivable that they could represent "weak spots" of the cell membrane through which the silver can penetrate. However, we cannot exclude that the silver artefactually penetrated the endothelial cell and secondarily created a myelin figure.

Of the 7 stigmata on the intercellular junctions one represented diapedesis, but 6 did not correspond to any recognizable, preexisting cellular pathology. Very small myelin figures arising from the overlying endothelium may have been artifacts. *Most of the silver was beneath the endothelium* (Fig. 10). We have previously shown evidence that the intercellular junction represents a pathway for small ions (including those of silver nitrate) (Zand et al. 1982); thus, a large subendothelial silver deposit beneath a junctional area is best interpreted as the effect of an *increased passage of silver ions through a segment of the junction.* In other words, these small spots along junctions could represent "physiological leaks". This is in keeping with known facts: Hüttner et al. (1973) found that the interendothelial junctions of the normal rat aorta vary in their permeability to horseradish peroxidase; some junctions are impermeable to the marker, others are not. Unfortunately the treatment with silver nitrate destroys the finer details of ultrastructure, thus it is not possible to tell whether the local junction was of the more patent type (it can not be patent enough to allow the escape of plasma proteins, because we never found focal deposits that could be interpreted in this manner).

Diapedesis in our material occurred only once; it was nearly completed, and the tail end of the monocyte produced a small stigma on an intercellular line (Fig. 11 b). *Ongoing* diapedesis gives rise to an intercellular stoma: a correlation that was already discussed by Cohnheim in his classic description of diapedesis (Cohnheim 1867). Therefore, combining our results with available data, we can suggest that *a stoma in a cell represents a myoendothelial hernia, a stoma along the junction represents diapedesis.* This statement will require further confirmation, because electron microscopic data on diapedesis are scanty. Traditionally, diapedesis is believed to occur between cells; however, in a study of lightly injured venous endothelium, Stehbens (1965, Fig. 10) illustrated several typical intracellular stomata, each one containing the nucleus of a leukocyte, as if the latter were performing transcellular diapedesis. We made similar observations in a study of hypercholesterolemic rats (to be published). It is therefore possible that – in apparent contrast with the current dogma for the microcirculation (and inflammation) – diapedesis at the level of *aortic* endothelium may sometimes take place also across the body of an endothelial cell. This type of transcellular diapedesis is thought to occur physiologically in the bone marrow (De Bruyn et al. 1977) and also in the high endothelial venules of lymphatic organs (Farr and De Bruyn 1975).

To conclude: in our study of *normal* rat aorta we found that 17 stomata/stigmata could be explained – at the cellular level – in at least 4 different ways. More ways could surely be found if the same approach were extended to pathologic arteries. Some of the mechanisms here described (particularly diapedesis and the myoendothelial herniae) can be considered, strictly speaking, abnormal, but they are constant events in the normal rat aorta (Joris et al. 1979; Stetz et al. 1979).

If our findings are combined with the few data available in the literature, the overall significance of stomata and stigmata in normal aortic endothe-

CELLULAR SIGNIFICANCE
OF STIGMATA AND STOMATA
IN THE RAT AORTA

STOMA in the cell		(I) Myo-endothelial hernia
STIGMA in the cell		(I) Myo-endothelial hernia (2) Bleb or myelin figure (3) Artifact (?)
STOMA on junction		(I) Diapedesis *
STIGMA on junction		(I) Point of higher permeability (2) Nearly completed diapedesis

Fig. 13. Cellular significance of stomata and stigmata examined by electron microscopy in the present study, and (*) proposed in the literature but not confirmed by electron microscopy

lium can be summarized as shown in Fig. 13. Clearly, these ancient Greek terms remain useful for descriptive purposes, although they have -- at the cellular level – a variety of meanings.

References

Altschul R (1954) Endothelium. Its development, morphology, function, and pathology. The MacMillan Company, New York

Björkerud S, Hansson H-A, Bondjers G (1972) Subcellular valves and canaliculi in arterial endothelium and their equivalence to so-called stigmata. Virchows Arch [Cell Pathol] 11:19–23

Caplan BA, Gerrity RG, Schwartz CJ (1974) Endothelial cell morphology in focal area of *in vivo* Evans blue uptake in the young pig aorta. I. Quantitative light microscopic findings. Exp Mol Pathol 21:102–117

Cohnheim J (1867) Über Entzündung und Eiterung. Arch Pathol Anat Physiol Klin Med 40:1–79

De Bruyn PPH, Becker RP, Michelson S (1977) The transmural migration and release of blood cells in acute myelogenous leukemia. Am J Anat 149:247–168

Edanaga M (1974) A scanning electron microscope study on the endothelium of the vessels. I. Fine structure of the endothelial surface of aorta and some other arteries in normal rabbits. Arch Histol Jpn 37:1–14

Fallon JT, Stehbens WE (1973) The endothelium of experimental saccular aneurysms of the abdominal aorta in rabbits. Br J Exp Pathol 54:13–19

Farr AG, De Bruyn PPH (1975) The mode of lymphocyte migration through postcapillary venule endothelium in lymph node. Am J Anat 143:59–92

Gertz SD, Forbes MS, Sunaga T, Kawamura J, Rennels ML, Shimamoto T, Nelson E (1976) Ischemic carotid endothelium. Transmission electron microscopic studies. Arch Pathol Lab Med 100:522–526

Gordon D, Guyton JR, Karnovsky MJ (1981) Intimal alterations in rat aorta induced by stressful stimuli. Lab Invest 45:14–27

Gregorius FK, Rand RW (1975) Scanning electron microscopic observations of common carotid artery endothelium in the rat. I. Crater artifacts. Surg Neurol 4:252–257

Hoff HF, Gottlob R (1967) A fine structure study of injury to the endothelial cells of the rabbit abdominal aorta by various stimuli. Angiology 18:440–451

Hüttner I, Boutet M, Rona G, More RH (1973) Studies on protein passage through arterial endothelium. III. Effect of blood pressure levels on the passage of fine structural protein tracers through rat arterial endothelium. Lab Invest 29:536–546

Joris I, Stetz E, Majno G (1979) Lymphocytes and monocytes in the aortic intima. An electron study in the rat. Atherosclerosis 34:221–231

Joris I, Zand T, Majno G (1982) Hydrodynamic injury of the endothelium in acute aortic stenosis. Am J Pathol 106:394–408

Joris I, Zand T, Nunnari JJ, Krolikowski FJ, Majno G (1983) Studies on the pathogenesis of atherosclerosis. I. Adhesion and emigration of mononuclear cells in the aorta of hypercholesterolemic rats. Am J Pathol 113:341–358

Leak LV, Rahil K (1978) Permeability of the diaphragmatic mesothelium. The ultrastructural basis for "stomata". Am J Anat 151:557–593

Mironov VA, Gusev SA, Baradi AF (1979) Mesothelial stomata overlying omental milky spots: Scanning electron microscopic study. Cell Tissue Res 201:327–330

Silkworth JB, McLean B, Stehbens WE (1975) The effect of hypercholesterolemia on aortic endothelium studied en face. Atherosclerosis 22:335–348

Stadtmüller F (1921) Historische Darstellung zur Deutung des Wesens der Silber Methode an nicht fixierten Objekten. Anat Hefte 59:79–210

Stehbens WE (1965) Reaction of venous endothelium to injury. Lab Invest 14:449–459

Stetz EM, Majno G, Joris I (1979) Cellular pathology of the rat aorta. Pseudo-vacuoles and myo-endothelial herniae. Virchows Arch [Pathol Anat] 383:135–148

Tsilibary EC, Wissig SL (1983) Lymphatic absorption from the peritoneal cavity: Regulation of patency of mesothelial stomata. Microvasc Res 25:22–39

Zand T, Underwood JM, Nunnari JJ, Majno G, Joris I (1982) Endothelium and "silver lines". An electron microscopic study. Virchows Arch [Pathol Anat] 395:133–144